Istituto Nazionale di Fisica Nucleare
Sezione di Bari

INFN/AE-76/7
17 Maggio 1976

C. Favuzzi, G. Maggi and F. Waldner: A FEASIBILITY STUDY FOR A FOCUSSING SINGLE ARM SPECTROMETER AT $p_{inc} \geqslant 400$ GeV/c. -

This note is part of a project of feasibility study for a Focussing Single Arm Spectrometer (FSAS from now on) for the SPS at CERN supported by INFN under project No. SP3.

1. - INTRODUCTION. -

A FSAS has to be intended more as a general purpose device than a single experiment oriented apparatus. Working with a high resolution unseparated beam, and measuring two 4--momenta (p_{inc} and p_{out}), the apparatus is especially suitable to explore (in the "low t" region) fields as elastic scattering, two body and quasi-two-body reactions, inclusive reactions. The apparatus can therefore cover by itself a large portion of high energy physics: it can be made more versatile if additional equipment around the target is used.

Principal advantages of the instrument are the high event rates; the possibility (more precisely: the necessity) of an on-line connection of the whole set up; the experimental data in digital form on tapes; the simplicity of the data reduction stage; the high statistics easily achievable; the small dimensions of the detectors owing to the small beam size.

Schematically the apparatus can be sketched as in Fig. 1.

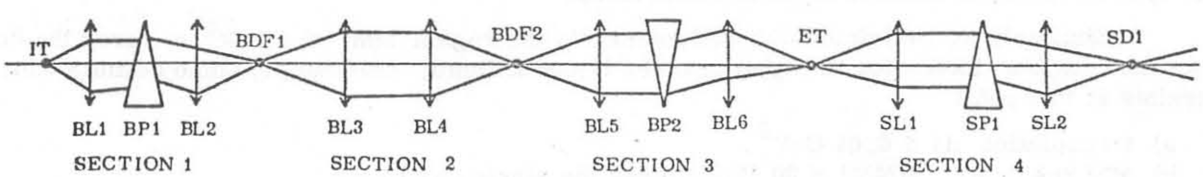

FIG. 1

The circulating beam strikes the internal target (IT) and gives rise to an unseparated beam which enters the beam line through a lens (quadrupole triplet, normally) BL1, a prism of magnetic dipoles (BP1), and another lens BL2: in this way one gets a first dispersed focus BDF1. The beam is transported farther away through a couple of lenses BL3 and BL4. At

BDF2 there is a second dispersed focus that can truly analyze the momentum (in BDF1 one is usually too near to the hot zone of the accelerator). A second system BL5, BP2, BL6, symmetric with the first section focusses the beam recombining the various momenta on the external target (ET) (liquid H_2 or D_2, normally). Through the whole beam line, detectors are placed to give the transverse (x, y) coordinates of the incoming particles. In this way one can have p_x, p_y, p_z at the interaction point at ET. Cerenkov counters or other detectors must give also the mass of the incoming particle : in this way the equipment can give the incoming 4-momentum.

A similar structure in the spectrometer arm (SL1, SP1, SL2) allows one measure the outgoing 4-momentum. To explore different angular regions in low energy experiments one usually rotates the spectrometer arm (SA) : in the hundred of GeV region this is unthinkable owing to the tremendous length of the apparatus, combined with the painstaking accuracy of the alignment. One usually uses therefore a magnetic bending of the incoming beam, leaving the SA stationary. This bending is done usually "into the ground" for obvious safety reasons.

In this note we describe possible layouts that can work up to 400 or 500 GeV/c of incoming momentum : in designing these layouts we followed closely the design philosophy of the FSAS at FNAL.

2. - GENERAL REQUIREMENTS. -

The FSAS analyzes a reaction like

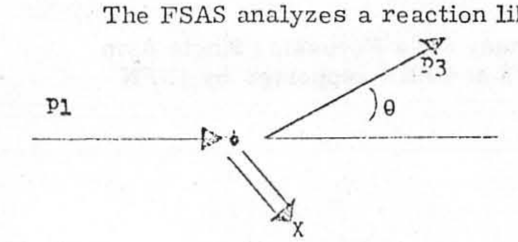

$$\begin{array}{lll} \pi p \to \pi x & K p \to \pi x & p p \to \pi x \\ \quad\ \to K x & \quad\ \to K x & \quad\ \to K x \\ \quad\ \to p x & \quad\ \to p x & \quad\ \to p x . \end{array}$$

in all charges combinations : there are also similar reactions with the neutron as target. These inclusive reactions can be described with 2 variables : (t, MM) is a most popular choice (together with (p_T, ξ_L) or even scaled variables) whereas (p_3, θ) are the variables given by our apparatus (see ref. (2)).

We restricted our apparatus to explore regions not farther than t = -3 GeV^2 (i.e. after the first diffraction bump), taking advantage of the fact that the cross section at t = - 1 is nearly equal to that at t = - 3.

The geometrical acceptance is going down, however, so we do think that a reasonable choice will be t = - 1 GeV^2 as the maximum t that can be reached with a reasonable signal to noise ratio. This parameter is not essential, however, as it's more or less a matter of brute force to bend the beam enough to reach high t values.

On the other side (small t values) we think that the FNAL limit (0.05 GeV^2) is more or less an intrinsic limit of the instrument itself.

Similarly we restricted our equipment into the region MM^2 $\lesssim$ 9 GeV^2 to cover the resonance region. Extension to higher masses is not difficult. One can put some definite constraints at this point

a) t resolution $\Delta t \lesssim 0.01$ GeV^2,
b) MM resolution Δ(MM) $\lesssim$ 80 MeV (to see the single pion),
c) positive identification of the masses (incoming and outgoing).

These constraints are easily translated into lab variables : we can in fact observe that in the range previously defined t is essentially a function of θ only and MM is a function of (p_1 - p_3) only. If we approximate t with the formula

$$t \simeq - p_{inc}^2 \ \psi_{lab}^2 ,$$

where ψ_{lab} is the angle of scattering in lab system, we get:

$$\Delta\psi_{lab} \simeq \frac{\Delta t}{2p\sqrt{-t}} ,$$

which with $\Delta t = -0.01$ becomes:

$$\Delta\psi_{lab} \simeq \frac{0.05}{p\sqrt{-t}} ,$$

which can be computed at the limits :

$$t = -0.05 \qquad \text{to} \qquad t = -1 .$$

Similarly we have (t very small, $m_{inc} \simeq 1$ GeV):

$$\Delta(MM) \simeq \Delta(p_1 - p_3) ,$$

with these rough estimates of our resolutions in mind, we obtain ($\Delta\psi$ in μrad, $\Delta\delta$ in percent with $\delta = \dfrac{p_1 - p_3}{p_1} \times 100$) :

$\Delta\psi_{lab}$	from	224	to	50	at	100 GeV/c	$\Delta\delta = \frac{\Delta p}{p} \times 100$	0.08 at	100 GeV/c
		112		25		200		0.04	200
		74		17		300		0.0273	300
		56		12		400		0.02	400
		45		10		500		0.016	500
		37		8		600		0.013	600

Taking into account also the finite resolution of the BA, these limits have to be tightened by roughly a factor of 2, posing therefore a very severe series of constraints on the inherent precision of the equipment especially on the magnification and dispersion at the dispersed foci.

These requirements are summarized in Figs. 2, 3, (graphs for $\Delta\psi_{lab}$ and $\Delta\delta$ as functions of p_{inc}).

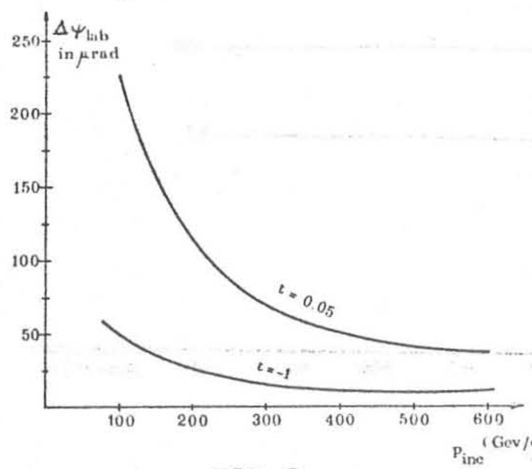

FIG. 2

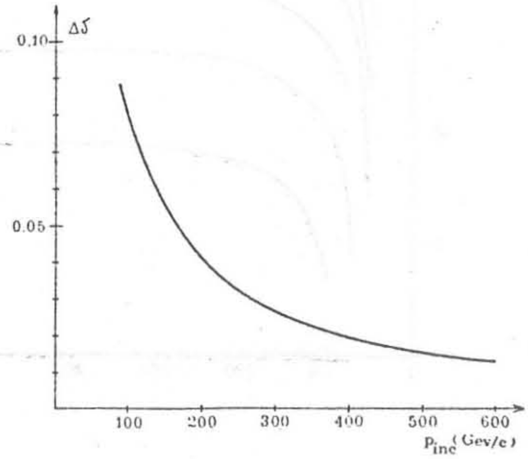

FIG. 3

Another requirement is an excellent beam parallelism in the parallel sections if one wants to use Cerenkov counters. We can see the situation in Figs. from 4 to 7. The parallelism should be guaranteed within one half of the πK separation.

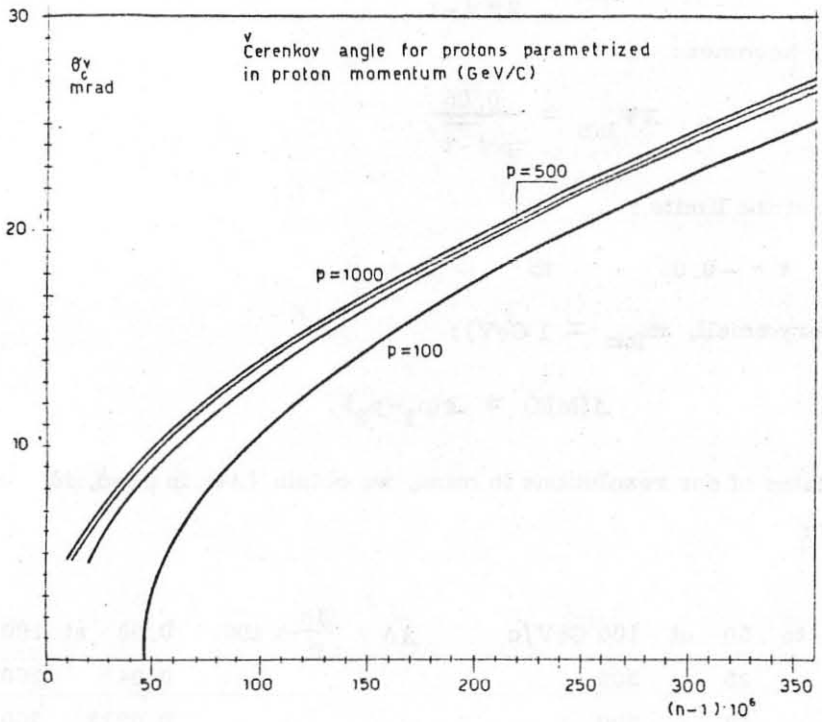

FIG. 4

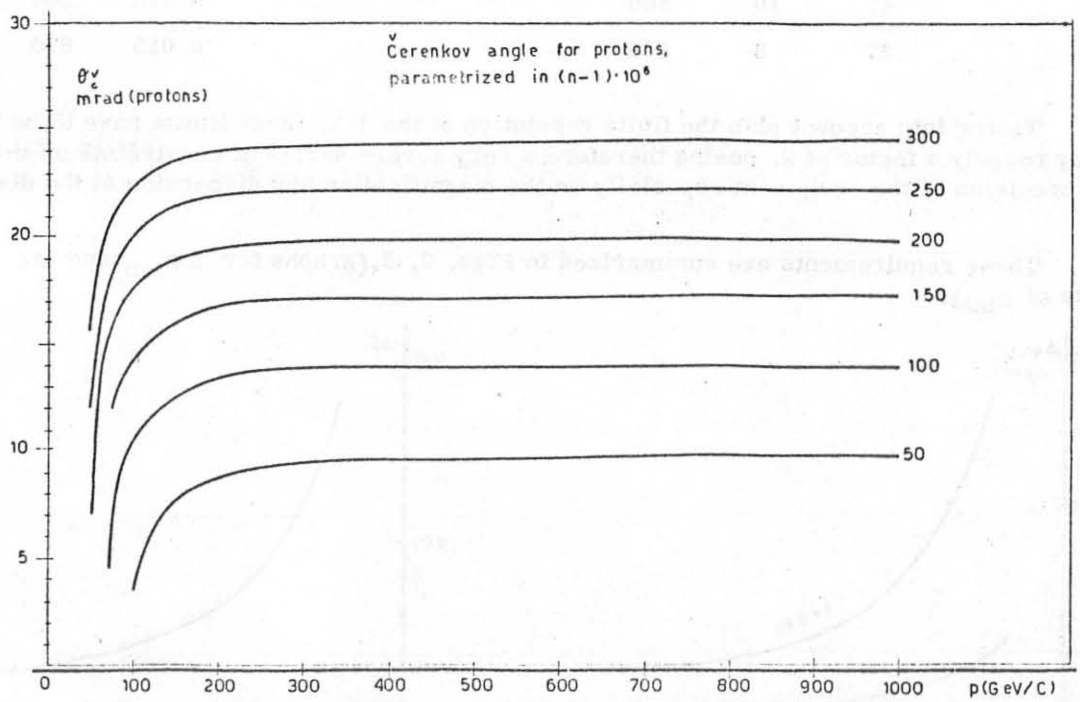

FIG. 5

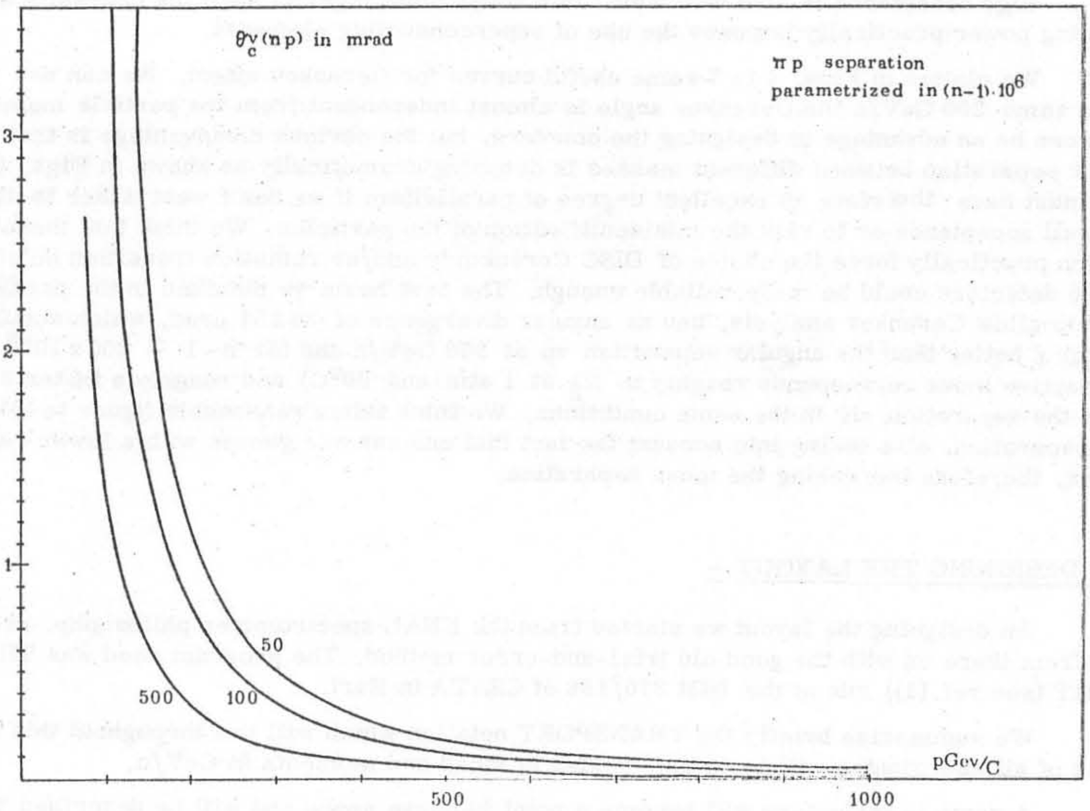

θ^V_c(π p) in mrad
π p separation
parametrized in $(n-1)\cdot 10^6$
3
2
1
50
500
100
pGev/C
500
1000

FIG. 6

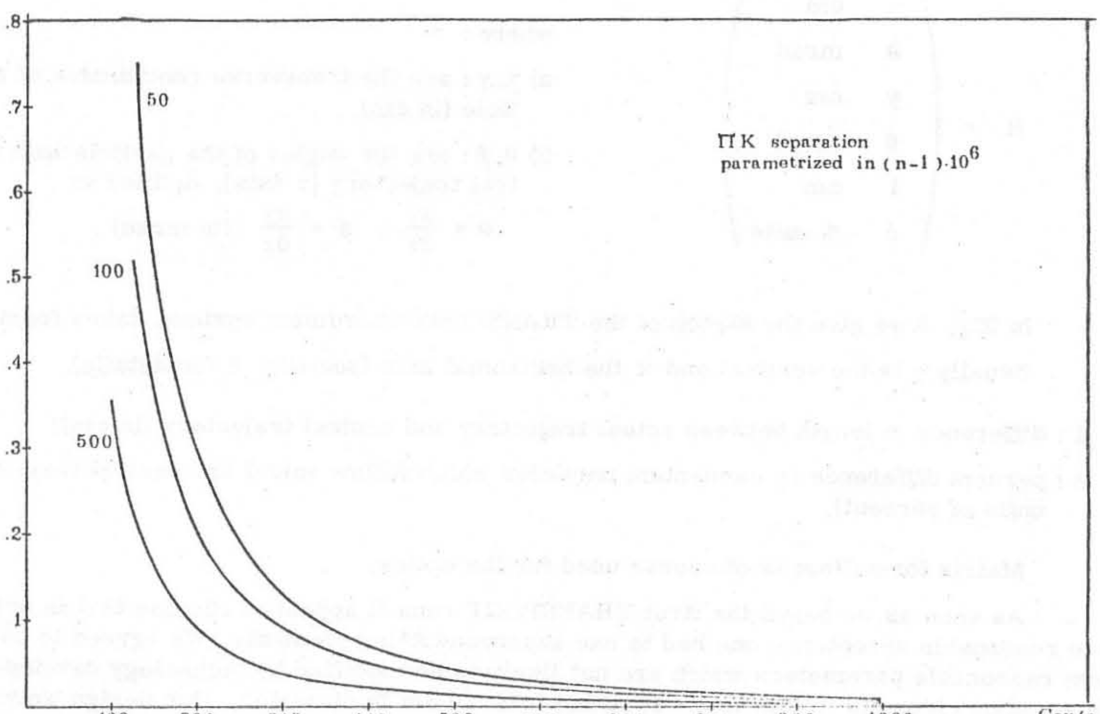

.8
.7
.6
.5
.4
.3
.2
.1
50
100
500
Π K separation
parametrized in $(n-1)\cdot 10^6$
100
200
300
400
500
600
700
800
900
1000
p
Gev/c

FIG. 7

High acceptance is also desirable : this constraints together with the necessity of a high bending power practically imposes the use of superconducting elements.

We plotted in Figs. 4 to 7 some useful curves for Cerenkov effect. We can see that over some 200 GeV/c the Cerenkov angle is almost independent from the particle momentum : this can be an advantage in designing the counters, but the obvious disadvantage is that the angular separation between different masses is dropping dramatically as shown in Figs. 6 and 7. We must have therefore an excellent degree of parallelism if we don't want either to drop the overall acceptance or to risk the misidentification of the particles. We think that these consideration practically force the choice of DISC Cerenkov's and/or radiation transition detectors, if these detectors could be made reliable enough. The best beam we obtained in the parallel section to allow Cerenkov analysis, has an angular divergence of 36×51 μrad, which should be a factor 6 better than the angular separation πp at 500 GeV/c and for $n-1 \simeq 300 \times 10^{-6}$ (This refractive index corresponds roughly to N_2 at 1 atm and $20^{o}C$) and roughly a factor 2 better than the separation πK in the same conditions. We think this a reasonable figure to allow π-K--p separation, also taking into account the fact that one can use gasses with a lower refractive index, therefore increasing the mass separation.

3. - DESIGNING THE LAYOUT. -

In designing the layout we started from the FNAL spectrometer philosophy, proceeding from there on with the good old trial-and-error method. The program used was TRANSPORT (see ref. (1)) run at the IBM 370/158 of CSATA in Bari.

We summarize briefly the TRANSPORT notation which will use throughout this note : first of all coordinates will be in cm, angles in mrad and momenta in GeV/c.

A particle trajectory will become a point in phase space and will be described by a vector :

$$R = \begin{pmatrix} x & \text{cm} \\ \theta & \text{mrad} \\ y & \text{cm} \\ \phi & \text{mrad} \\ 1 & \text{cm} \\ \delta & \%\ \text{units} \end{pmatrix}$$

where :

a) x, y : are the transverse coordinates of the particle (in cm).

b) θ, ϕ : are the angles of the particle with the central trajectory (z axis), defined as

$$\theta = \frac{dy}{dz} \; ; \quad \phi = \frac{dy}{dz} \quad \text{(in mrad)} .$$

In Fig. 8 we give the sketch of the TRANSPORT coordinate system, taken from ref. (1).

Usually y is the vertical and x the horizontal axis (see Fig. 8 for details).

c) 1 : difference in length between actual trajectory and central trajectory (in cm);

δ : percent difference in momentum particles which follow actual and central trajectories (in units of percent).

Matrix formalism is of course used for the optics.

As soon as we begun the first TRANSPORT runs it appeared obvious that in order to have reasonable acceptance one had to use superconducting elements. We agreed to use for them reasonable parameters which are not likely to be modified by technology development. We stood on elements 1.2 m long with a hot hole 10 cm in diameter. Our design works at 400 GeV/c if 4 T are reached. Higher momenta with no layout modifications can be reached with higher fields.

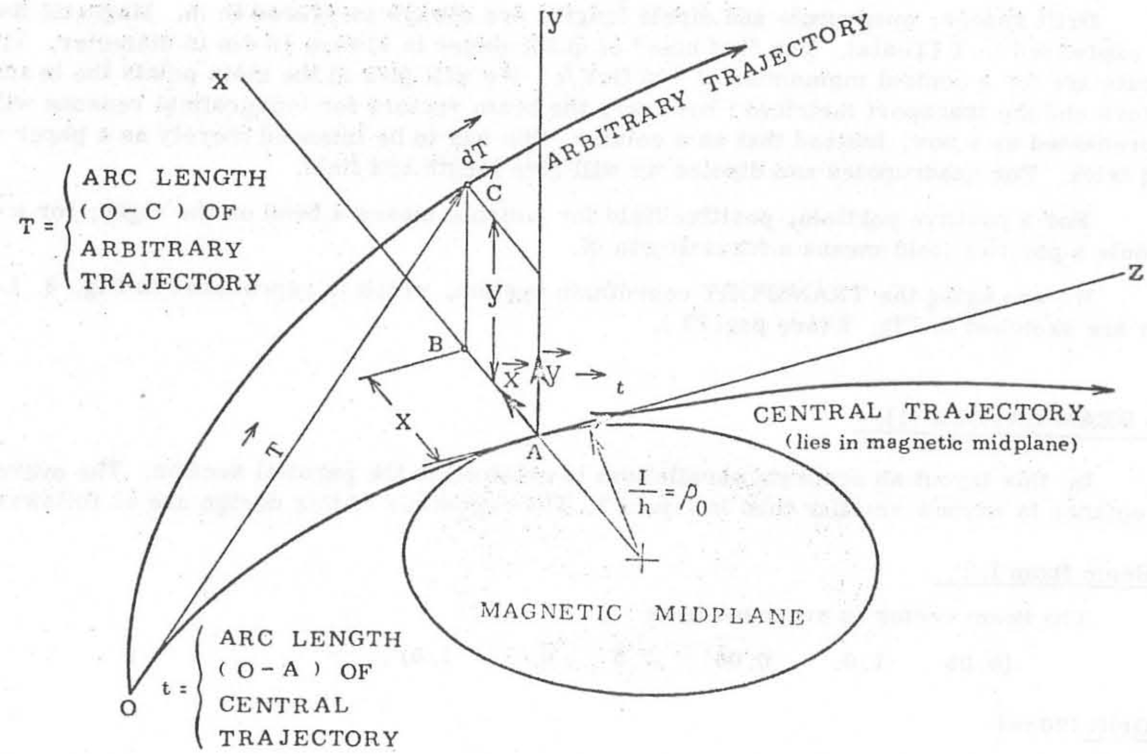

FIG. 8 - Curvilinear coordinate system used in derivation of equation motion.

The constraints on the instrument we kept in mind are :

1) To have available as much phase space as possible.
2) To have suitable parallelism in the parallel sections in order to allow Cerenkov analysis (other detectors as the transition radiation counters would ease this constraint).
3) To have a resolution $\Delta t \leq 0.01$ GeV^2, Δ(MM) $\leq$ 80 MeV with a 2 mm separation, at least at the SA dispersed focus (this allows the use of standard MWPC).
4) To limit as much as possible the number of elements and the overall length of the system.
5) To have a reasonable clearance around the secondary target.

For what point 4) is concerned we can roughly sketch what we can expect for the total bending power (in T. m) scaling up the FNAL solution.

	FNAL (180 GeV/c)	400 GeV/c	600 GeV/c
quadrupoles	13.7	30.4	45.7
dipoles	46.0	102.2	153.3
	59.7	132.7	199.0

This would allow the same resolution in $\Delta p/p$, which corresponds to a worsening of the situation for Δp and therefore on Δ(MM).

We give in the following sections the essentials of the various layouts we obtained. The notation used in the TRANSPORT notation, both for the beam vectors and for the transport matrices.

Drift spaces, quadrupole and dipole lengths are always measured in m. Magnetic fields are expressed in T (Tesla). The "hot hole" of quadrupoles is always 10 cm in diameter. The layouts are for a central momentum of 400 GeV/c. We will give at the main points the beam vectors and the transport matrices : however, the beam vectors for typografical reasons will be presented as a row, instead that as a column : this has to be intended merely as a paper saving trick. For quadrupoles and dipoles we will give length and field.

For a positive particle, positive field for a dipole means a bend on the right ; for a quadrupole a positive field means a focussing in X.

We are using the TRANSPORT coordinate system, which is reproduced in Fig. 8. Layouts are sketched in Fig. 9 (see pag. 23).

4. - BEAM LAYOUT (1). -

In this layout an accurate parallelism is obtained in the parallel section. The overall acceptance is anyhow smaller than in layout 2. The essentials of this design are as follows :

1) Beam from I. T.

The beam vector is supposed to be :

(0.05 1.0 0.05 1.5 0. 1.0) .

2) Drift (20 m)

3) Triplet lens BL1

a) Quadrupole (2.4 m, 2.263 T)
b) Drift (1 m)
c) Quadrupole (2.4 m, - 1.42 T)
d) Drift (1 m)
e) Quadrupole (2.4 m, - 1.42 T)
f) Drift (1 m)
g) Quadrupole (2.4 m, - 1.42 T)
h) Drift (1 m)
i) Quadrupole (2.4 m, 2.263 T).

At this point the beam vector is :

(3.360 0.015 3.870 0.019 0.0 1.0)

and the transport matrix is :

$$\begin{pmatrix} 0.595 & 3.364 & 0. & 0. & 0. & 0. \\ -2.297 & 2\text{x}10^{-5} & 0. & 0. & 0. & 0. \\ 0. & 0. & 0.775 & 2.579 & 0. & 0. \\ 0. & 0. & -0.388 & 5\text{x}10^{-5} & 0. & 0. \\ 0. & 0. & 0. & 0. & 1. & 0. \\ 0. & 0. & 0. & 0. & 0. & 1. \end{pmatrix}$$

4) Drift (15 m)

5) Dispersive section BP1

This is a set of 10 dipoles each 2 m long and with a field of 4 T, rotated from the optical axis of 0.17 degrees (i.e. of the correct amount) and separated from next dipole by a drift of 0.5 m.

After this section the beam vector is :

(3.449 0.600 3.860 0.021 0.202 1.0)

and the transport matrix is :

$$\begin{pmatrix} -0.595 & 3.363 & 0. & 0. & 0. & 0.764 \\ -0.297 & 8\times10^{-5} & 0. & 0. & 0. & 0.600 \\ 0. & 0. & -0.775 & 2.573 & 0. & 0. \\ 0. & 0. & -0.387 & -0.004 & 0. & 0. \\ 0.129 & -0.202 & 0. & 0. & 1. & -0.015 \\ 0. & 0. & 0. & 0. & 0. & 1. \end{pmatrix}$$

6) Drift (1 m)

7) Triplet lens BL2

a) Quadrupole (2.4 m, - 5.323 T)
b) Drift (1 m)
c) Quadrupole (2.4 m, 2.281 T)
d) Drift (1 m)
e) Quadrupole (2.4 m, 2.281 T)
f) Drift (1 m)
g) Quadrupole (2.4 m, 2.281 T)
h) Drift (1 m)
i) Quadrupole (2.4 m, - 5.323 T).

At this point the beam vector is :

(3.307 0.798 4.884 1.047 0.202 1.0)

and the transport matrix is :

$$\begin{pmatrix} -0.8076 & 3.068 & 0. & 0. & 0. & 1.232 \\ -0.140 & -0.705 & 0. & 0. & 0. & 0.374 \\ 0. & 0. & 0.176 & -3.256 & 0. & 0. \\ 0. & 0. & 0.269 & 0.698 & 0. & 0. \\ 0.013 & -0.202 & 0. & 0. & 1. & -0.015 \\ 0. & 0. & 0. & 0. & 0. & 1. \end{pmatrix}$$

8) Dispersive section BP2

After a 1 m drift follows a section of 5 dipoles with the same characteristics as the BP1 dipoles.

9) Drift (30 m)

We have here the first dispersed horizontal focus (DHF1) where the beam vector is :

(3.954 0.975 0.322 1.05 0.286 1.0)

and the transport matrix is :

$$\begin{pmatrix} -1.418 & 6\times10^{-4} & 0. & 0. & 0. & 3.953 \\ -0.140 & -0.705 & 0. & 0. & 0. & 0.674 \\ 0. & 0. & 1.347 & -0.21 & 0. & 0. \\ 0. & 0. & 0.269 & 0.700 & 0. & 0. \\ 0.04 & -0.279 & 0. & 0. & 1. & -0.06 \\ 0. & 0. & 0. & 0. & 0. & 1. \end{pmatrix}$$

After 3 m we have the first vertical dispersed focus (DVF1) with the following beam vector:

(4.053 0.688 0.073 1.023 0.286 1.00)

and the following transport matrix :

$$\begin{pmatrix} -1.42 & -0.208 & 0. & 0. & 0. & 4.047 \\ 0.118 & -0.686 & 0. & 0. & 0. & -0.053 \\ 0. & 0. & 1.465 & -0.003 & 0. & 0. \\ 0. & 0. & 0.519 & 0.682 & 0. & 0. \\ 0.04 & -0.28 & 0. & 0. & 1. & -0.06 \\ 0. & 0. & 0. & 0. & 0. & 1. \end{pmatrix}$$

A field lens (a quadrupole 1.2 m long, with a field of 1.0 T and a hot hole of 10 cm in diameter) between the two foci does not change anything in the optics, but does improve the overall down-stream acceptance of the system.

10) Drift (15 m)

11) Triplet lens BL3

a) Quadrupole (2.4 m, 2.404 T)
b) Drift (1 m)
c) Quadrupole (2.4 m, - 1.532 T)
d) Drift (1 m)
e) Quadrupole (2.4 m, - 1.532 T)
f) Drift (1 m)
g) Quadrupole (2.4 m, - 1.532 T)
h) Drift (1 m)
i) Quadrupole (2.4 m, 2.404 T).

At this point the beam vector is :

(3.052 1.258 2.115 0.036 0.286 1.000)

and the transport matrix is :

$$\begin{pmatrix} -0.433 & -2.22 & 0. & 0. & 0. & 2.098 \\ 0.45 & 10^{-5} & 0. & 0. & 0. & -1.258 \\ 0. & 0. & 2.136 & 1.408 & 0. & 0. \\ 0. & 0. & -0.710 & 3\times10^{-5} & 0. & 0. \\ 0.04 & -0.279 & 0. & 0. & 1.0 & -0.062 \\ 0. & 0. & 0. & 0. & 0. & 1.0 \end{pmatrix}$$

12) Drift (10 m)

At this point the beam vector is :

(2.371 1.258 2.113 0.036 0.286 1.000)

A larger drift can be used if required, and this will not decrease the acceptance : in this case the layout from this point on has to be changed if one wants to maintain the same optical properties.

13) Triplet lens BL4

a) Quadrupole (2.4 m, 2.461 T)
b) Drift (1 m)
c) Quadrupole (2.4 m, - 1.517 T)
d) Drift (1 m)
e) Quadrupole (2.4 m, - 1.517 T)
f) Drift (1 m)
g) Quadrupole (2.4 m, - 1.517 T)
h) Drift (1 m)
i) Quadrupole (2.4 m, 2.461 T)

At this point the beam vector is :

(2.601 1.186 1.607 0.895 0.286 1.000)

and the transport matrix is :

$$\begin{pmatrix} 1.003 & -1.122 & 0. & 0. & 0. & -2.346 \\ 0.222 & 0.748 & 0. & 0. & 0. & -0.920 \\ 0. & 0. & 0.3778 & 1.072 & 0. & 0. \\ 0. & 0. & -1.143 & -0.595 & 0. & 0. \\ 0.04 & -0.279 & 0. & 0. & 1.0 & -0.062 \\ 0. & 0. & 0. & 0. & 0. & 1.0 \end{pmatrix}$$

14) Drift (15 m)

The beam vector is here :

(3.727 1.186 0.276 0.895 0.286 1.00)

and we have the second dispersed horizontal focus (DHF2) with the following transport matrix :

$$\begin{pmatrix} 1.336 & 10^{-5} & 0. & 0. & 0. & -3.727 \\ 0.222 & 0.748 & 0. & 0. & 0. & -0.920 \\ 0. & 0. & -1.337 & 0.179 & 0. & 0. \\ 0. & 0. & -1.143 & -0.595 & 0. & 0. \\ 0.040 & -0.279 & 0. & 0. & 1. & 0. \\ 0. & 0. & 0. & 0. & 0. & 1. \end{pmatrix}$$

After a drift of 3 m we have the second dispersed vertical focus (DVF2) with the following beam vector :

(3.906 0.763 0.086 0.872 0.286 1.000)

and the following transport matrix :

$$\begin{pmatrix} 1.366 & 0.222 & 0. & 0. & 0. & -3.899 \\ -0.023 & 0.728 & 0. & 0. & 0. & -0.228 \\ 0. & 0. & -1.720 & 0.002 & 0. & 0. \\ 0. & 0. & -1.415 & -0.579 & 0. & 0. \\ 0.04 & -0.279 & 0. & 0. & 1.0 & -0.062 \\ 0. & 0. & 0. & 0. & 0. & 1.0 \end{pmatrix}$$

15) Drift (15 m)

16) Triplet lens BL5

a) Quadrupole (2.4 m, 2.398 T)
b) Drift (1 m)
c) Quadrupole (2.4 m, - 1.530 T)
d) Drift (1 m)
e) Quadrupole (2.4 m, - 1.530 T)
f) Drift (1 m)
g) Quadrupole (2.4 m, - 1.530 T)
h) Drift (1 m)
i) Quadrupole (2.4 m, 2.398 T).

17) Dispersive section BP3

This section consists of 10 dipoles with the same characteristics as the previous ones, but with reversed field. After these dipoles we have a series of 8 more dipoles each 2 m long with a field of -4.681 T, tilted of 0.17 degrees with respect to the optical axis. The tilt is not what it should be if one wants to have the dipole symmetrically placed on the optical axis: this is done on purpose to take advantage of the focusing edge effect of a dipole.

18) Drift (20 m)

This is the "parallel section" mentioned before, in which one can analyze the beam with Cerenkov counters.

The beam vector is :

(2.559 0.036 1.626 0.051 0.161 1.000)

and we can see that we have here an excellent parallelism (36 x 51 μrad). The transport matrix is :

$$\begin{pmatrix} -2.127 & 2.557 & 0. & 0. & 0. & 0.003 \\ -0.413 & 0.026 & 0. & 0. & 0. & -0.014 \\ 0. & 0. & 1.886 & -1.082 & 0. & 0. \\ 0. & 0. & 0.894 & 0.017 & 0. & 0. \\ -0.003 & 0.0036 & 0. & 0. & 1. & -0.161 \\ 0. & 0. & 0. & 0. & 0. & 1. \end{pmatrix}$$

19) Triplet lens BL6

a) Quadrupole (2.4 m, 1.936 T)
b) Drift (1 m)
c) Quadrupole (2.4 m, -2.218 T)
d) Drift (1 m)
e) Quadrupole (2.4 m, -2.218 T)

f) Drift (1 m)
g) Quadrupole (2.4 m, -2.218 T)
h) Drift (1 m)
i) Quadrupole (2.4 m, 1.936 T).

20) Drift (30 m)

At this point we can put the external target: we have here in fact the recombined vertical and horizontal focus.

The beam vector is :

(0.101 0.612 0.168 0.447 0.161 1.000)

and the transport matrix is :

$$\begin{pmatrix} -1.635 & 0.00001 & 0. & 0. & 0. & -0.059 \\ 0.237 & -0.612 & 0. & 0. & 0. & -0.010 \\ 0. & 0. & 3.360 & 0. & 0. & 0. \\ 0. & 0. & 0.260 & 0.298 & 0. & 0. \\ -0.003 & 0.004 & 0. & 0. & 1. & 0.161 \\ 0. & 0. & 0. & 0. & 0. & 1. \end{pmatrix}$$

5. - BEAM LAYOUT (2). -

In this layout we obtained a reasonable, but not extreme degree of parallelism in the parallel section. We have a higher acceptance with respect to layout (1) and we think this as a reasonable design for the beam arm of an FSAS in which - for instance - transition radiation detectors instead of Cerenkov counters could be used.

1) Beam from internal target

(0.05 1.0 0.05 1.5 0. 1.0)

2) Drift (20 m)

3) Triplet lens BL1

a) Quadrupole (3.6 m, -1.576 T)
b) Drift (1 m)
c) Quadrupole (2.4 m, 1.441 T)
d) Drift (1 m)
e) Quadrupole (2.4 m, 1.446 T)
f) Drift (1 m)
g) Quadrupole (2.4 m, 1.441 T)
h) Drift (1 m)
i) Quadrupole (3.6 m, -1.576 T).

The beam vector is now :

(2.537 0.170 5.030 0.336 0. 1.0)

and the transport matrix :

$$\begin{pmatrix} 0.715 & 2.537 & 0. & 0. & 0. & 0. \\ -0.442 & -0.169 & 0. & 0. & 0. & 0. \\ 0. & 0. & 0.430 & 3.353 & 0. & 0. \\ 0. & 0. & -0.327 & -0.224 & 0. & 0. \\ 0. & 0. & 0. & 0. & 1.0 & 0. \\ 0. & 0. & 0. & 0. & 0. & 1.0 \end{pmatrix}$$

4) Drift (10 m)

5) Dispersive section BP1

This is a set of dipoles with field of 4. 0 T covering a total length of 40 m. The dipoles are tilted of the correct amount with respect to the optical axis.

The beam vector becomes now :

(2. 934   1. 213   3. 320   0. 350   0. 262   1. 00)

and the transport matrix :

$$\begin{pmatrix} -1.490 & 1.693 & 0. & 0. & 0. & 2.395 \\ -0.442 & -0.169 & 0. & 0. & 0. & 1.200 \\ 0. & 0. & -1.205 & 2.213 & 0. & 0. \\ 0. & 0. & -0.325 & -0.233 & 0. & 0. \\ -0.073 & -0.244 & 0. & 0. & 1.0 & -0.096 \\ 0. & 0. & 0. & 0. & 0. & 1.0 \end{pmatrix}$$

6) Drift (15 m)

7) Triplet lens BL2

a) Quadrupole (3. 6 m, 3. 259 T)
b) Drift (1 m)
c) Quadrupole (2. 4 m, -2. 036 T)
d) Drift (1 m)
e) Quadrupole (2. 4 m, -2. 036 T)
f) Drift (1 m)
g) Quadrupole (2. 4 m, -2. 036 T)
h) Drift (1 m)
i) Quadrupole (3. 6 m, 3. 259 T)

8) Drift (40 m)

At this point we have the two dispersed foci :

a) horizontal dispersed focus DHF1

Beam vector :

(4. 504   0. 747   0. 212   0. 548   0. 262   1. 000)

Transport matrix :

$$\begin{pmatrix} 1.847 & 0.00006 & 0. & 0. & 0. & -4.503 \\ 0.0489 & 0.541 & 0. & 0. & 0. & -0.515 \\ 0. & 0. & -2.684 & 0.110 & 0. & 0. \\ 0. & 0. & -0.185 & -0.365 & 0. & 0. \\ 0.073 & -0.244 & 0. & 0. & 1.0 & -0.096 \\ 0. & 0. & 0. & 0. & 0. & 1.0 \end{pmatrix}$$

b) after a drift of 3 m we have the first dispersed vertical focus DVF1 with this beam vector :

(4.661 0.747 0.137 0.548 0.262 1.0)

and the transport matrix :

$$\begin{pmatrix} 1.862 & 0.162 & 0. & 0. & 0. & -4.657 \\ 0.0489 & 0.541 & 0. & 0. & 0. & 0.515 \\ 0. & 0. & -2.739 & 0.0003 & 0. & 0. \\ 0. & 0. & -0.185 & -0.365 & 0. & 0. \\ 0.073 & -0.244 & 0. & 0. & 1. & -0.096 \\ 0. & 0. & 0. & 0. & 0. & 1. \end{pmatrix}$$

10) Drift (15 m)

11) Triplet lens BL3

a) Quadrupole (2.4 m, 2.404 T)
b) Drift (1 m)
c) Quadrupole (2.4 m, -1.531 T)
d) Drift (1 m)
e) Quadrupole (2.4 m, -1.531 T)
f) Drift (1 m)
g) Quadrupole (2.4 m, -1.531 T)
h) Drift (1 m)
i) Quadrupole (2.4 m, 2.404 T).

After this lens the beam vector is :

(4.524 1.396 1.139 0.066 0.262 1.00)

and the transport matrix is :

$$\begin{pmatrix} 1.188 & 1.747 & 0. & 0. & 0. & -4.173 \\ -0.572 & 0. & 0. & 0. & 0. & 1.395 \\ 0. & 0. & -2.368 & -0.755 & 0. & 0. \\ 0. & 0. & 1.324 & 0. & 0. & 0. \\ 0.073 & -0.244 & 0. & 0. & 1. & -0.096 \\ 0. & 0. & 0. & 0. & 0. & 1. \end{pmatrix}$$

12) Drift (20 m)

13) Triplet lens BL4

a) Quadrupole (2.4 m, 2.404 T)
b) Drift (1 m)
c) Quadrupole (2.4 m, -1.531 T)
d) Drift (1 m)
e) Quadrupole (2.4 m, -1.531 T)
f) Drift (1 m)
g) Quadrupole (2.4 m, -1.531 T)
h) Drift (1 m)
i) Quadrupole (2.4 m, 2.404 T).

14) Drift (15 m)

Here we have the second dispersed horizontal focus DHF2 with the beam vector :

(4.145 1.323 0.137 0.549 0.262 1.000)

and the transport matrix :

$$\begin{pmatrix} -1.747 & 0.162 & 0. & 0. & 0. & 4.140 \\ -0.333 & -0.541 & 0. & 0. & 0. & 1.207 \\ 0. & 0. & 2.740 & 3\text{x}10^{-5} & 0. & 0. \\ 0. & 0. & 0.824 & 0.365 & 0. & 0. \\ 0.073 & -0.244 & 0. & 0. & 1. & -0.096 \\ 0. & 0. & 0. & 0. & 0. & 1. \end{pmatrix}$$

After a drift of 3 m we have the second dispersed vertical focus DVF2 where the beam vector is :

(4.503 1.323 0.222 0.549 0.262 1.0)

and the transport matrix is :

$$\begin{pmatrix} -1.847 & 0. & 0. & 0. & 0. & 4.502 \\ -0.333 & -0.541 & 0. & 0. & 0. & 1.207 \\ 0. & 0. & 2.988 & 0.109 & 0. & 0. \\ 0. & 0. & 0.824 & 0.365 & 0. & 0. \\ 0.073 & -0.244 & 0. & 0. & 1. & -0.096 \\ 0. & 0. & 0. & 0. & 0. & 1. \end{pmatrix}$$

15) Drift (3 m)

16) Triplet lens BL5

a) Quadrupole (2.4 m, 2.767 T)
b) Drift (1 m)
c) Quadrupole (2.4 m, -1.688 T)
d) Drift (1 m)
e) Quadrupole (2.4 m, -1.688 T)
f) Drift (1 m)
g) Quadrupole (2.4 m, -1.688 T)
h) Drift (1 m)
i) Quadrupole (2.4 m, 2.767 T).

The beam vector is now :

(5.100 1.704 1.025 0.074 0.262 1.000)

with the following transport matrix :

$$\begin{pmatrix} -1.578 & -1.431 & 0. & 0. & 0. & 4.893 \\ 0.699 & 10^{-5} & 0. & 0. & 0. & -1.703 \\ 0. & 0. & 3.451 & 0.674 & 0. & 0. \\ 0. & 0. & -1.484 & 10^{-5} & 0. & 0. \\ 0.073 & -0.244 & 0. & 0. & 1. & -0.096 \\ 0. & 0. & 0. & 0. & 0. & 1. \end{pmatrix}$$

17) Drift (3 m)

18) Dispersive section BP2

This is a line of dipoles for a total length of 30 m. The field is -5.373 T. The tilt with respect to the optical axis is $1^{\circ}.7$, to take advantage of the focussing edge effects.

19) Triplet lens BL6

a) Quadrupole (3.6 m, 3.230 T)
b) Drift (1 m)
c) Quadrupole (2.4 m, -2.048 T)
d) Drift (1 m)
e) Quadrupole (2.4 m, -2.048 T)
f) Drift (1 m)
g) Quadrupole (2.4 m, -2.048 T)
h) Drift (1 m)
i) Quadrupole (3.6 m, 3.230 T).

At this point the beam vector is :

(3.0 0.867 0.931 0.166 0.396 1.0)

with the following transport matrix :

$$\begin{pmatrix} 0.735 & 1.728 & 0. & 0. & 0. & -2.455 \\ -0.700 & -0.286 & 0. & 0. & 0. & 0.817 \\ 0. & 0. & -2.758 & 0.619 & 0. & 0. \\ 0. & 0. & -1.153 & -0.104 & 0. & 0. \\ 0.112 & -0.071 & 0. & 0. & 1. & -0.390 \\ 0. & 0. & 0. & 0. & 0. & 1. \end{pmatrix}$$

20) Drift (10 m)

21) Dispersive section BP3

This is a line of 40 m of dipoles with a field of -2.733 T, tilted 3° with respect to the optical axis. After an additional drift of 10 m we have the following beam vector :

(0.173 0.291 0.485 0.165 0.434 1.000)

and the transport matrix at this point (recombined horizontal and vertical focus) is :

$$\begin{pmatrix} -3.458 & 10^{-5} & 0. & 0. & 0. & 4\times10^{-5} \\ -0.695 & -0.289 & 0. & 0. & 0. & 10^{-5} \\ 0. & 0. & -9.704 & 2\times10^{-5} & 0. & 0. \\ 0. & 0. & -1.166 & -0.103 & 0. & 0. \\ 0. & -10^{-5} & 0. & 0. & 1. & -0.434 \\ 0. & 0. & 0. & 0. & 0. & 1. \end{pmatrix}$$

6. - SPECTROMETER ARM LAYOUT. -

In this layout we kept as high as possible the acceptance in θ and φ.

1) Beam from ET

(0.05 1.5 0.05 3.0 0. 1.)

2) Drift (5 m)

3) Triplet lens SL1

a) Quadrupole (1.2 m, 4.000 T)
b) Drift (6.07 m)
c) Quadrupole (1.2 m, -2.479 T)
d) Drift (1 m)
e) Quadrupole (1.2 m, -2.479 T)
f) Drift (1 m)
g) Quadrupole (1.2 m, -2.479 T)
h) Drift (6.07 m)
i) Quadrupole (1.2 m, 4.000 T).

At this point we have the beam vector :

(4.899 0.015 3.385 0.044 0. 1.)

and the transport matrix is :

$$\begin{pmatrix} 0.153 & 3.266 & 0. & 0. & 0. & 0. \\ -0.306 & 0.0001 & 0. & 0. & 0. & 0. \\ 0. & 0. & 0.444 & 1.128 & 0. & 0. \\ 0. & 0. & -0.866 & 0.0006 & 0. & 0. \\ 0. & 0. & 0. & 0. & 1. & 0. \\ 0. & 0. & 0. & 0. & 0. & 1. \end{pmatrix}$$

4) Drift (15 m)

5) Dispersive section SP1

This section consists of 20 dipoles each 2 m long with a field of 4 T. Each of them is rotated with respect the optical axis of 0.17 degrees. They are separated from each other by drifts of 0.5 m. The beam after this section is :

(5.73 1.20 3.38 0.04 0.6 1.0)

and the transport matrix is :

$$\begin{pmatrix} -1.82 & 3.27 & 0. & 0. & 0. & 2.97 \\ -0.306 & 0. & 0. & 0. & 0. & 1.199 \\ 0. & 0. & -5.25 & 1.12 & 0. & 0. \\ 0. & 0. & -0.875 & -0.003 & 0. & 0. \\ 0.127 & -0.39 & 0. & 0. & 1. & -0.119 \\ 0. & 0. & 0. & 0. & 0. & 1. \end{pmatrix}$$

6) Triplet lens SL2

a) Quadrupole (1.2 m, 2.756 T)
b) Drift (3 m)
c) Quadrupole (1.2 m, -1.764 T)
d) Drift (1 m)
e) Quadrupole (1.2 m, -1.764 T)
f) Drift (1 m)
g) Quadrupole (1.2 m, -1.764 T)
h) Drift (3 m)
i) Quadrupole (1.2 m, 2.756 T).

At this point the beam vector is :

(6.16 0.98 3.02 0.64 0.60 1.00)

and the transport matrix is :

$$\begin{pmatrix} -2.064 & 2.711 & 0. & 0. & 0. & 4.625 \\ 0.070 & -0.577 & 0. & 0. & 0. & 0.460 \\ 0. & 0. & -5.666 & 1.003 & 0. & 0. \\ 0. & 0. & 0.205 & -0.213 & 0. & 0. \\ 0.127 & -0.392 & 0. & 0. & 1. & -0.120 \\ 0. & 0. & 0. & 0. & 0. & 1. \end{pmatrix}$$

7) Dispersive section SP2

This section has 5 more dipoles, with the same characteristics as before. After a drift of 34.47 m we have the disperse focus of the spectrometer arm : the beam vector is here :

(8.00 1.15 0.23 0.64 0.74 1.00)

and the transport matrix is :

$$\begin{pmatrix} -1.733 & 0. & 0. & 0. & 0. & 8.00 \\ 0.07 & -0.577 & 0. & 0. & 0. & 0.76 \\ 0. & 0. & -4.683 & 0. & 0. & 0. \\ 0. & 0. & 0.21 & -0.213 & 0. & 0. \\ 0.188 & -0.462 & 0. & 0. & 1. & -0.269 \\ 0. & 0. & 0. & 0. & 0. & 1. \end{pmatrix}$$

The beam after this point is left free : at FNAL one has at this point a couple of Cerenkov threshold counters.

7. - RESOLUTION OF THE APPARATUS. -

a) New matrices

We give in this section some useful matrices that will allow the reader to transform a generic phase space point into the ET phase space.

The situation for the beam line is as follows : if x_1 is the beam vector at the internal target, x at an intermediate point in the beam line and x_o at the external target we have :

$$x = A x_1 , \qquad x_o = A_o x_1 ,$$

where A is the transport matrix, and therefore

$$x_o = A_o A^{-1} x = C x .$$

The matrix $C = A_o A^{-1}$ connects the beam vector with the down-stream external target.

The situation is simpler for the spectrometer arm. The generic beam vector x is connected with the ET phase space through the relation

$$x_o = A^{-1} x .$$

We give in the following the matrices $C = A_o A^{-1}$ computed for the most important points of the apparatus in both layouts, and the matrices A^{-1} for the spectrometer arm.

LAYOUT 1

From DHF1
$$\begin{pmatrix} 1.15302 & 0.00008 & 0.0 & 0.0 & -4.61696 \\ -0.25284 & 0.86806 & 0.0 & 0.0 & 0.40441 \\ 0.0 & 0.0 & 2.35344 & 0.70603 & 0.0 \\ 0.0 & 0.0 & 0.10190 & 0.45628 & 0.0 \\ 0.0 & 0.0 & 0.0 & 0.0 & 1.00000 \end{pmatrix}$$

From DVF1
$$\begin{pmatrix} 1.12311 & -0.34055 & 0.0 & 0.0 & -4.62227 \\ -0.09049 & 0.91956 & 0.0 & 0.0 & 0.40494 \\ 0.0 & 0.0 & 2.28995 & 0.01007 & 0.0 \\ 0.0 & 0.0 & 0.02264 & 0.43705 & 0.0 \\ 0.0 & 0.0 & 0.0 & 0.0 & 1.00000 \end{pmatrix}$$

From BL3
$$\begin{pmatrix} -0.00002 & -3.63335 & 0.0 & 0.0 & -4.62971 \\ 0.27568 & 0.79193 & 0.0 & 0.0 & 0.40787 \\ 0.0 & 0.0 & 0.00010 & -4.73209 & 0.0 \\ 0.0 & 0.0 & 0.21164 & 0.27052 & 0.0 \\ 0.0 & 0.0 & 0.0 & 0.0 & 1.00000 \end{pmatrix}$$

From BL4
$$\begin{pmatrix} -1.22380 & -1.83569 & 0.0 & 0.0 & -4.61888 \\ 0.31335 & -0.34816 & 0.0 & 0.0 & 0.40482 \\ 0.0 & 0.0 & -1.99819 & -3.60010 & 0.0 \\ 0.0 & 0.0 & 0.18582 & -0.16605 & 0.0 \\ 0.0 & 0.0 & 0.0 & 0.0 & 1.00000 \end{pmatrix}$$

From DHF2
$$\begin{pmatrix} -1.22381 & 0.00003 & 0.0 & 0.0 & -4.62010 \\ 0.31335 & -0.81819 & 0.0 & 0.0 & 0.40513 \\ 0.0 & 0.0 & -1.99898 & -0.60137 & 0.0 \\ 0.0 & 0.0 & 0.18589 & -0.44492 & 0.0 \\ 0.0 & 0.0 & 0.0 & 0.0 & 1.00000 \end{pmatrix}$$

From DVF2

$$\begin{pmatrix} -1.19081 & 0.36315 & 0.0 & 0.0 & -4.61917 \\ 0.15853 & -0.88900 & 0.0 & 0.0 & 0.40542 \\ 0.0 & 0.0 & -1.94795 & -0.00673 & 0.0 \\ 0.0 & 0.0 & 0.27148 & -0.51374 & 0.0 \\ 0.0 & 0.0 & 0.0 & 0.0 & 1.00000 \end{pmatrix}$$

From parallel section

$$\begin{pmatrix} -0.04247 & 4.17759 & 0.0 & 0.0 & -0.00039 \\ -0.24641 & 0.69520 & 0.0 & 0.0 & 0.00047 \\ 0.0 & 0.0 & 0.05716 & 3.63781 & 0.0 \\ 0.0 & 0.0 & -0.26216 & 0.84388 & 0.0 \\ 0.0 & 0.0 & 0.0 & 0.0 & 1.00000 \end{pmatrix}$$

<u>LAYOUT 2</u>

From DHF1

$$\begin{pmatrix} -1.87223 & 0.00023 & 0.0 & 0.0 & -8.43050 \\ -0.36214 & -0.53416 & 0.0 & 0.0 & -1.90581 \\ 0.0 & 0.0 & 3.54193 & 1.06738 & 0.0 \\ 0.0 & 0.0 & 0.40653 & 0.40471 & 0.0 \\ 0.0 & 0.0 & 0.0 & 0.0 & 1.00000 \end{pmatrix}$$

From DVF1

$$\begin{pmatrix} -1.87186 & 0.56054 & 0.0 & 0.0 & -8.42855 \\ -0.36207 & -0.42577 & 0.0 & 0.0 & -1.90544 \\ 0.0 & 0.0 & 3.54271 & 0.00286 & 0.0 \\ 0.0 & 0.0 & 0.40662 & 0.28253 & 0.0 \\ 0.0 & 0.0 & 0.0 & 0.0 & 1.00000 \end{pmatrix}$$

From BL3

$$\begin{pmatrix} 0.00001 & 6.04547 & 0.0 & 0.0 & -8.43336 \\ -0.16543 & 0.87146 & 0.0 & 0.0 & -1.90600 \\ 0.0 & 0.0 & -0.00003 & -7.32935 & 0.0 \\ 0.0 & 0.0 & 0.13642 & -0.63667 & 0.0 \\ 0.0 & 0.0 & 0.0 & 0.0 & 1.00000 \end{pmatrix}$$

From DHF2

$$\begin{pmatrix} 1.87252 & 0.56070 & 0.0 & 0.0 & -8.42894 \\ 0.28002 & 0.61805 & 0.0 & 0.0 & -1.90524 \\ 0.0 & 0.0 & -3.54171 & 0.00035 & 0.0 \\ 0.0 & 0.0 & -0.34069 & -0.28216 & 0.0 \\ 0.0 & 0.0 & 0.0 & 0.0 & 1.00000 \end{pmatrix}$$

From DVF2

$$\begin{pmatrix} 1.87223 & -0.00002 & 0.0 & 0.0 & -8.42873 \\ 0.27997 & 0.53420 & 0.0 & 0.0 & -1.26043 \\ 0.0 & 0.0 & -3.53913 & 1.05695 & 0.0 \\ 0.0 & 0.0 & -0.34044 & -0.18052 & 0.0 \\ 0.0 & 0.0 & 0.0 & 0.0 & 1.00000 \end{pmatrix}$$

From BL5

$$\begin{pmatrix} -0.00004 & -4.94716 & 0.0 & 0.0 & -8.42477 \\ 0.20195 & -0.53837 & 0.0 & 0.0 & -1.90498 \\ 0.0 & 0.0 & -0.00007 & 6.53893 & 0.0 \\ 0.0 & 0.0 & -0.15283 & 0.43032 & 0.0 \\ 0.0 & 0.0 & 0.0 & 0.0 & 1.00000 \end{pmatrix}$$

From BL6

$$\begin{pmatrix} 0.98677 & 5.96202 & 0.0 & 0.0 & -2.44840 \\ -0.00352 & 0.98921 & 0.0 & 0.0 & -0.81682 \\ 0.0 & 0.0 & 1.00870 & 6.00348 & 0.0 \\ 0.0 & 0.0 & 0.00250 & 1.00529 & 0.0 \\ 0.0 & 0.0 & 0.0 & 0.0 & 1.00000 \end{pmatrix}$$

SPECTROMETER ARM

From SL1
$$\begin{pmatrix} 0.00010 & -3.26792 & 0.0 & 0.0 & 0.0 \\ 0.30618 & 0.15309 & 0.0 & 0.0 & 0.0 \\ 0.0 & 0.0 & 0.00061 & -1.15442 & 0.0 \\ 0.0 & 0.0 & 0.88628 & 0.45440 & 0.0 \\ 0.0 & 0.0 & 0.0 & 0.0 & 1.00000 \end{pmatrix}$$

From SP1
$$\begin{pmatrix} 0.0 & -3.26797 & 0.0 & 0.0 & 3.91830 \\ 0.30581 & -1.81887 & 0.0 & 0.0 & 1.27257 \\ 0.0 & 0.0 & -0.00301 & -1.12478 & 0.0 \\ 0.0 & 0.0 & 0.87873 & -5.27241 & 0.0 \\ 0.0 & 0.0 & 0.0 & 0.0 & 1.00000 \end{pmatrix}$$

From SL2
$$\begin{pmatrix} -0.57633 & -2.70786 & 0.0 & 0.0 & 3.91116 \\ -0.06992 & -2.06161 & 0.0 & 0.0 & 1.27172 \\ 0.0 & 0.0 & -0.21274 & -1.00175 & 0.0 \\ 0.0 & 0.0 & -0.20475 & -5.65897 & 0.0 \\ 0.0 & 0.0 & 0.0 & 0.0 & 1.00000 \end{pmatrix}$$

From SP2
$$\begin{pmatrix} -0.57703 & 0.0 & 0.0 & 0.0 & 4.61627 \\ -0.07000 & -1.73310 & 0.0 & 0.0 & 1.87719 \\ 0.0 & 0.0 & -0.21354 & 0.0 & 0.0 \\ 0.0 & 0.0 & -0.21053 & -4.69484 & 0.0 \\ 0.0 & 0.0 & 0.0 & 0.0 & 1.00000 \end{pmatrix}$$

We give in Fig. 9 the block sketch of the layouts we obtained. In the following figures (10-18) we give the acceptance plots for the various layouts and experimental conditions.

b) The spectrometer arm

From the transport matrices of Sect. 7 we can write down the following formulas (where the subscript "o" refers to the external target) :

after SL1
$$X = 0.153\,X_o + 3.266\,\theta_o$$
$$Y = 0.444\,Y_o + 1.128\,\phi_o$$

after SP1
$$X = -1.82\,X_o + 3.27\,\theta_o + 2.97\,\delta_o$$
$$Y = -5.25\,Y_o + 1.12\,\phi_o$$

after SL2
$$X = -2.064\,X_o + 2.711\,\theta_o + 4.625\,\delta_o$$
$$Y = -5.666\,Y_o + 1.003\,\phi_o$$

after SP2
$$X = -1.733\,X_o + 8.00\,\delta_o$$
$$Y = -4.683\,Y_o\,.$$

We see therefore that we can compute θ_o, ϕ_o, δ_o and X_o, Y_o which at any rate have to be intended as a small correction to the overall situation. The system of equations is overdetermined. In particular the measurement of δ is best done at the focus : taking into account the fact that $|X_o| \leq 0.05$ we have at the focus

$$\Delta X = 1.733 \times 0.05 + 8 \times \Delta\delta\ ,$$

as a "worst case".

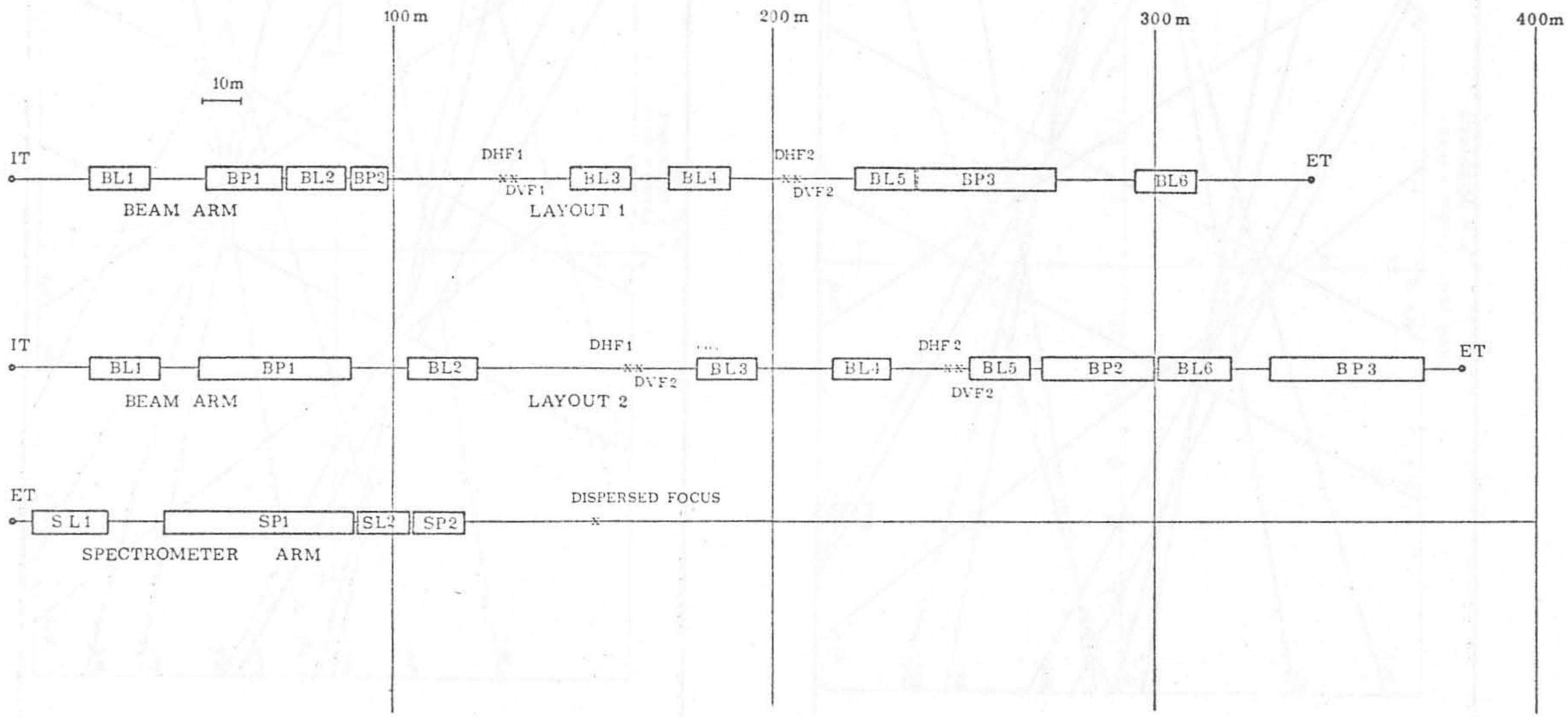
100 m
200 m
300 m
400m
10m
IT
BL1
BP1
BL2
BP2
DHF1
DVF1
BL3
BL4
DHF2
DVF2
BL5
BP3
BL6
ET
BEAM ARM
LAYOUT 1
IT
BL1
BP1
BL2
DHF1
DVF2
BL3
BL4
DHF2
DVF2
BL5
BP2
BL6
BP3
ET
BEAM ARM
LAYOUT 2
ET
SL1
SP1
SL2
SP2
DISPERSED FOCUS
SPECTROMETER ARM

FIG. 9

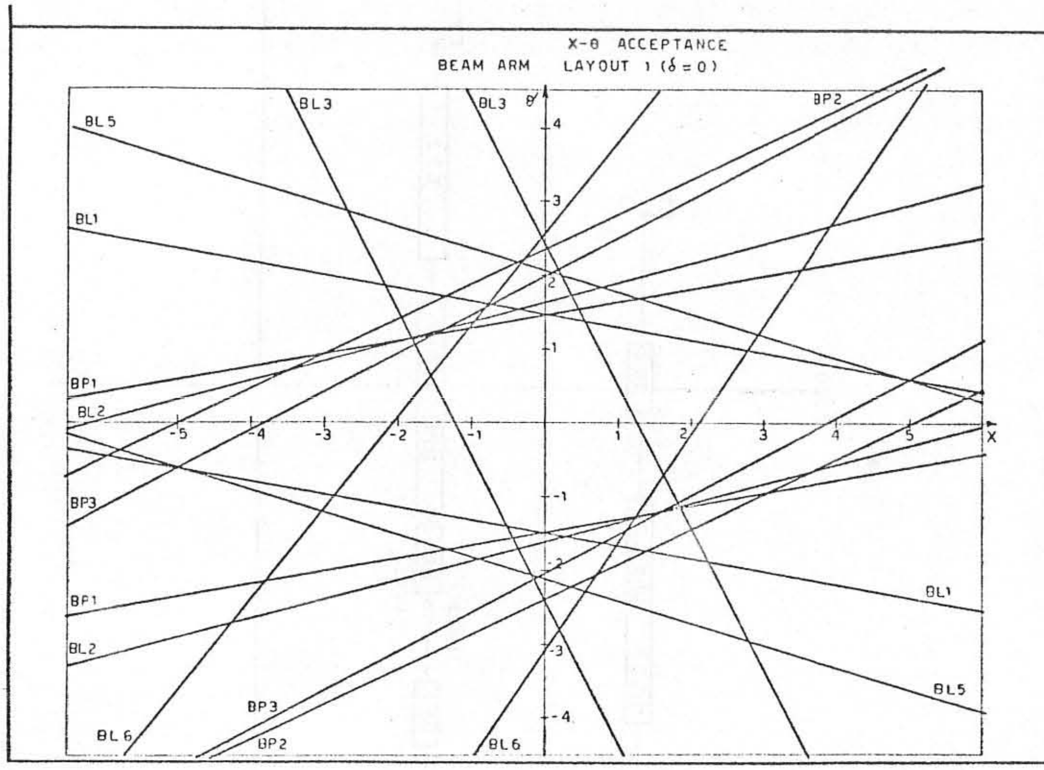

X-θ ACCEPTANCE
BEAM ARM LAYOUT 1 (δ = 0)
BL5
BL1
BP1
BL2
BP3
BL3
BP2
BL6
θ
X

FIG. 10

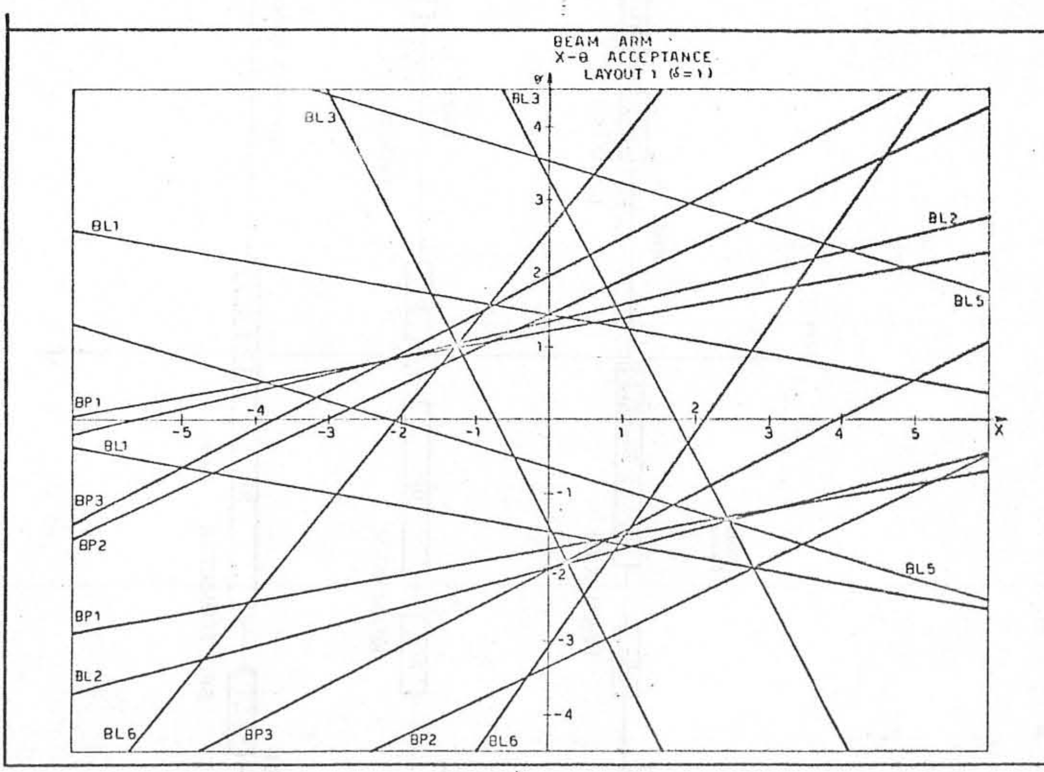

BEAM ARM
X-θ ACCEPTANCE
LAYOUT 1 (δ = 1)
BL1
BP1
BP3
BP2
BL2
BL3
BL5
BL6
θ
X

FIG. 11

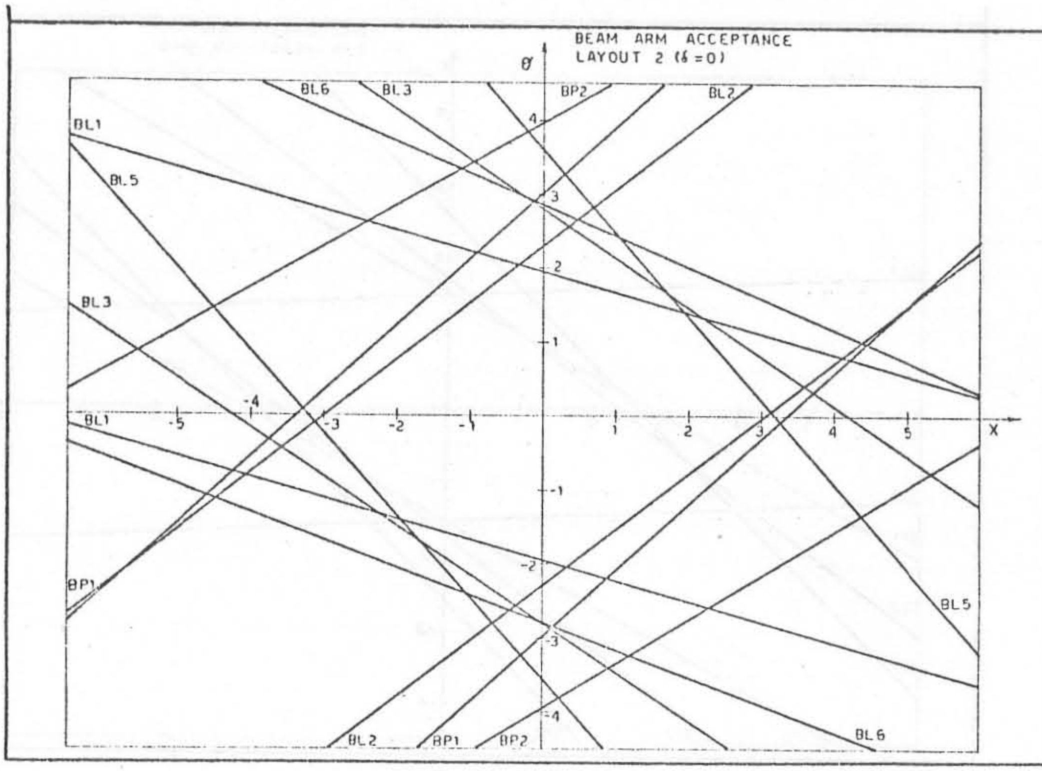

FIG. 12

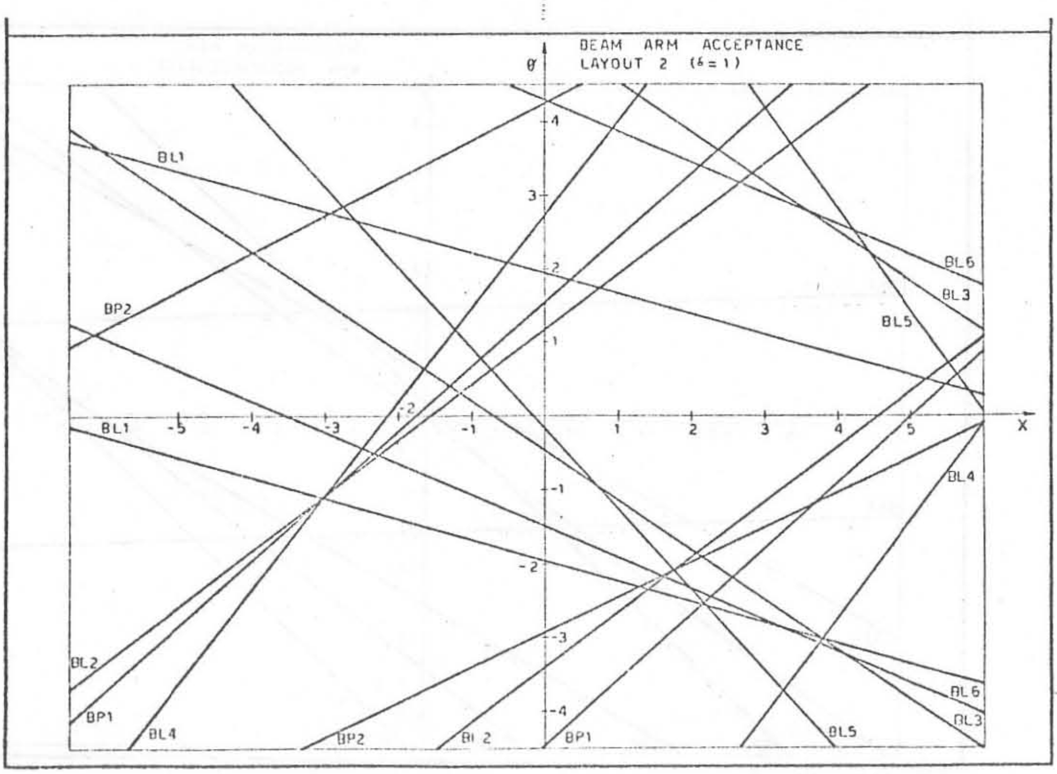

FIG. 13

427

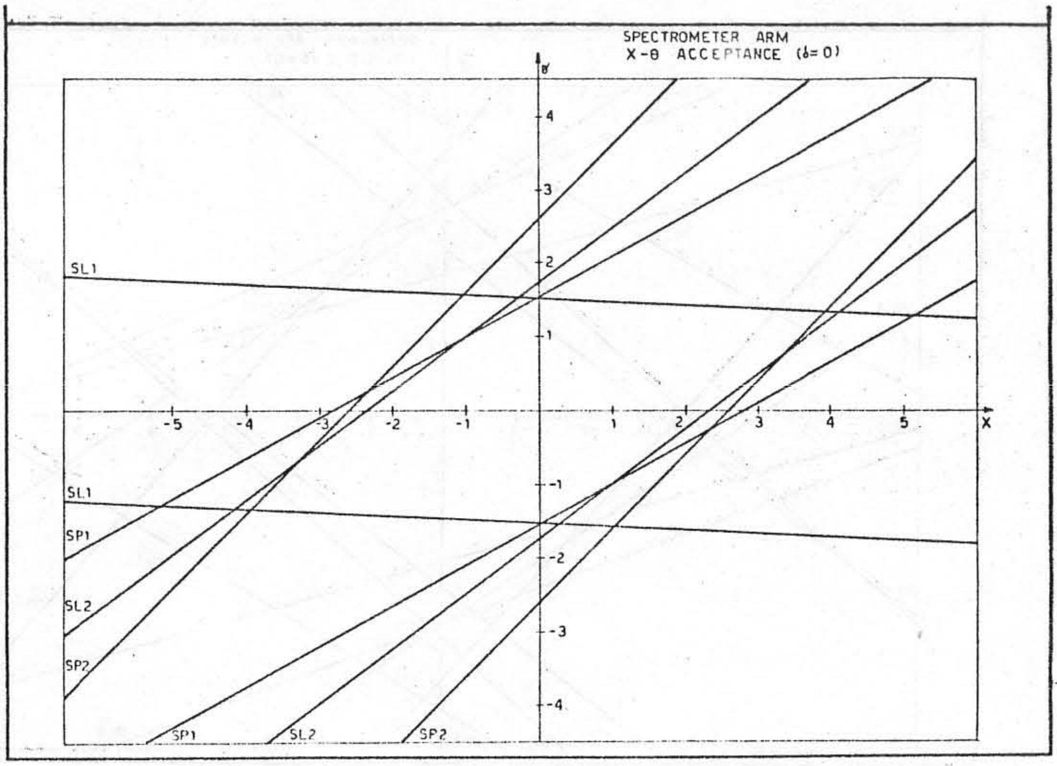
SPECTROMETER ARM
X-θ ACCEPTANCE (δ=0)
θ
4
3
2
1
-1
-2
-3
-4
-5
-4
-3
-2
-1
1
2
3
4
5
X
SL1
SL1
SP1
SL2
SP2
SP1
SL2
SP2

FIG. 14

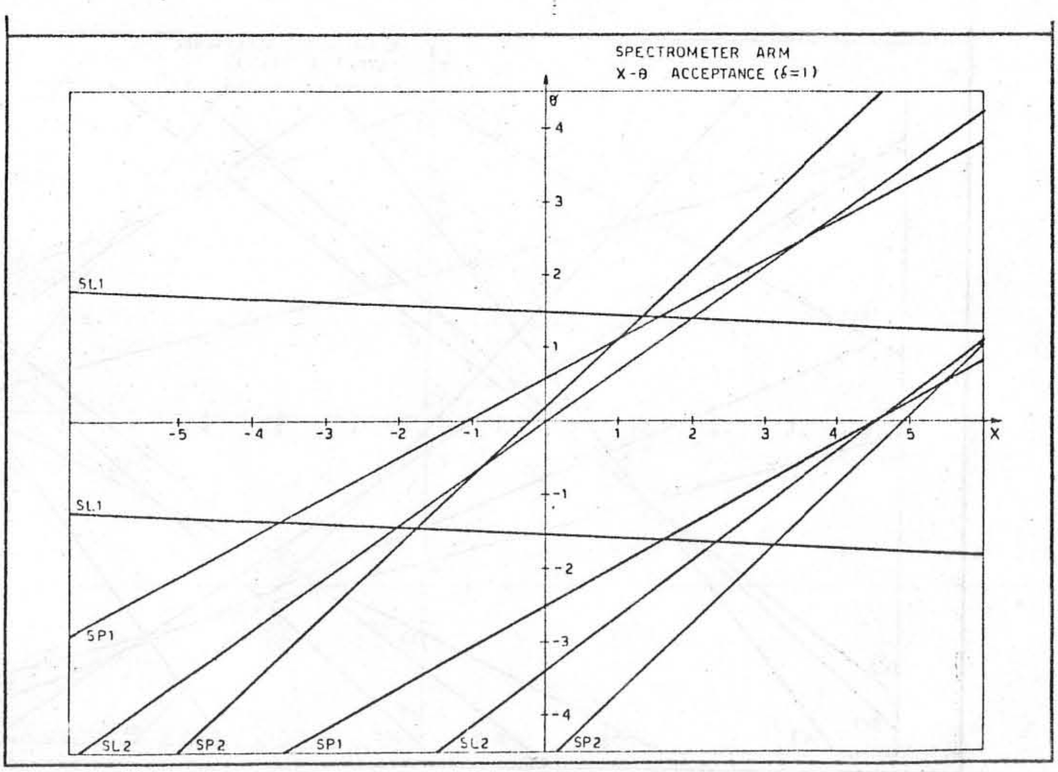
SPECTROMETER ARM
X-θ ACCEPTANCE (δ=1)
θ
4
3
2
1
-1
-2
-3
-4
-5
-4
-3
-2
-1
1
2
3
4
5
X
SL1
SL1
SP1
SL2
SP2
SP1
SL2
SP2

FIG. 15

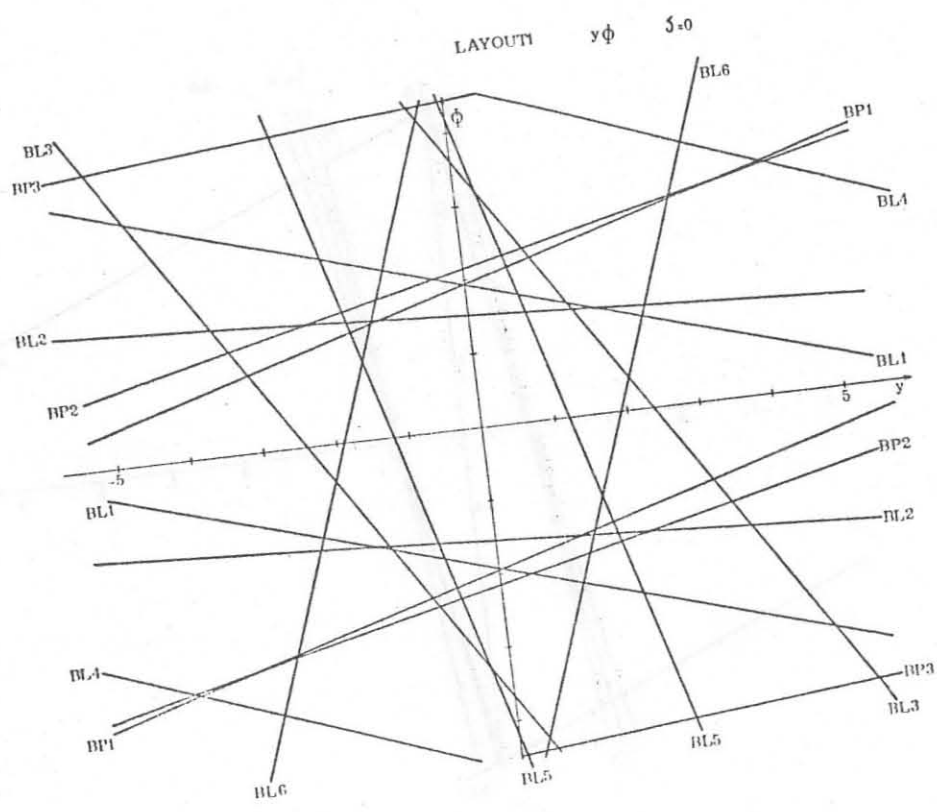
LAYOUT1 yφ δ=0
φ
y
5
-5
BL1
BL2
BL3
BL4
BL5
BL6
BP1
BP2
BP3

FIG. 16

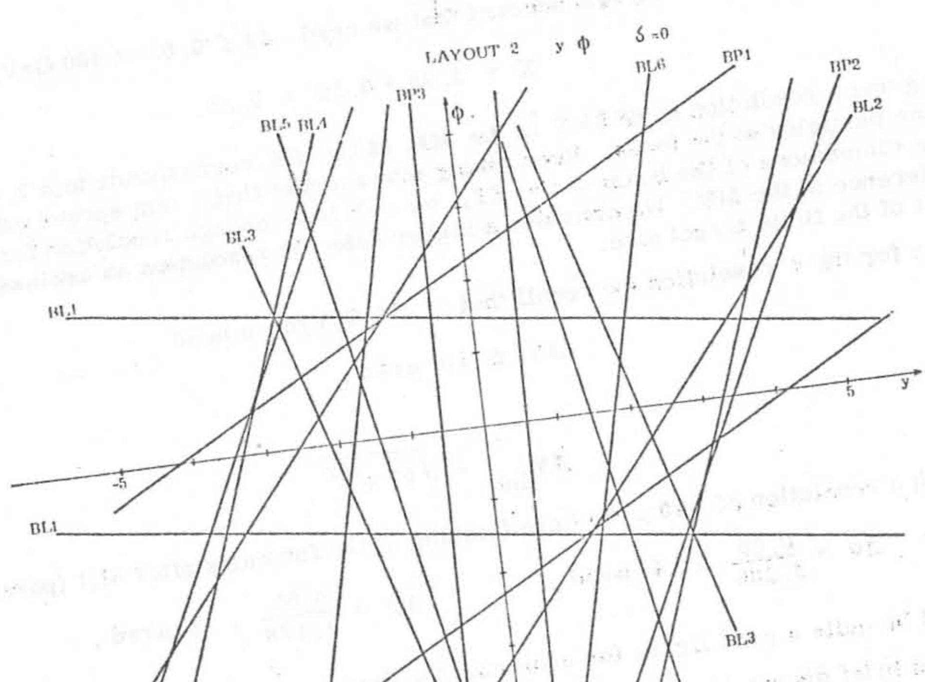
LAYOUT 2 y φ δ=0
φ
y
5
-5
BL1
BL2
BL3
BL4
BL5
BL6
BP1
BP2
BP3

FIG. 17

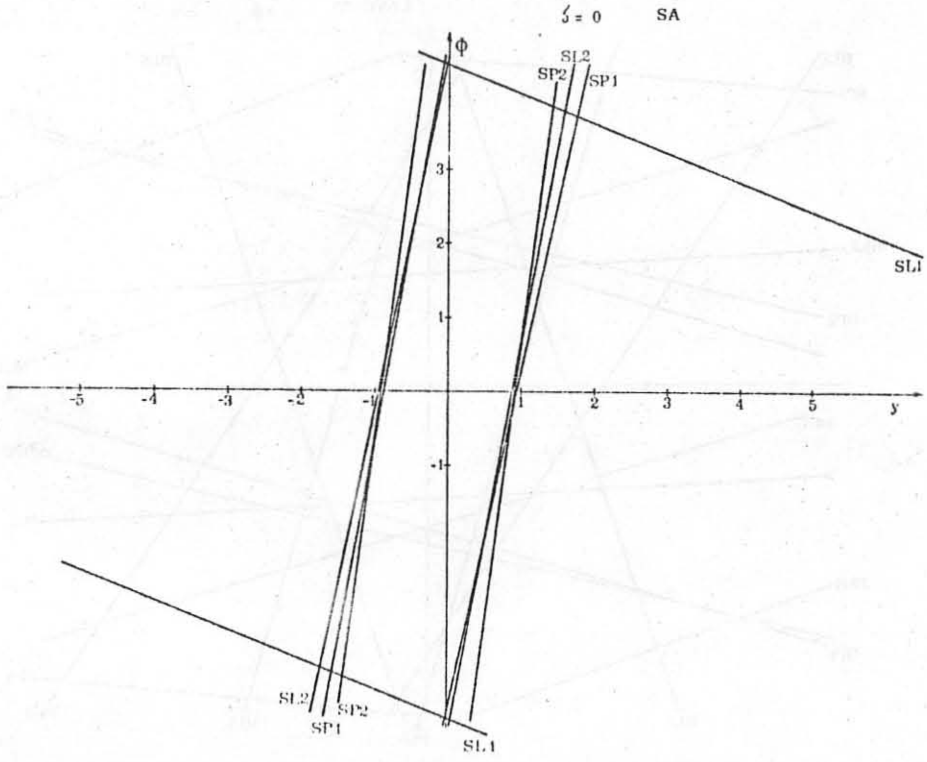

FIG. 18

This relation, taking into account that we need $\Delta\delta \leq 0.02$ at 400 GeV/c becomes :

$$X = 0.09 + 0.16 = 0.25 .$$

Summing up : a resolution of 80 MeV in the MM at the ET corresponds to a 2.5 mm separation of the particles at the focus. Even taking into account that 1 mm spread can come from the finite dimensions of the beam at the ET, we still have enough resolution for reading an 80 MeV difference in the MM. We consider a higher detector resolution as useless, just because the effect of the finite target size.

As for the t resolution we recall that at 400 GeV/c we need

$$\Delta\psi \leqslant 13 \ \mu\text{rad} ,$$

and that

$$\Delta\psi_{\text{lab}} = \sqrt{\theta^2 + \phi^2} .$$

With a resolution of 100 μ we have (looking at the formulas after SL1 (parallel section)):

$$\Delta\theta = \frac{0.05}{3.266} = 4 \ \mu\text{rad} , \qquad \Delta\phi = \frac{0.05}{1.128} = 8 \ \mu\text{rad} ,$$

which should be quite a good figure for achieving the desired t resolution.

In this brief discussion we didn't make any attempt of using the X_o Y_o contribution, which can always be computed from the above formulas, and is small in any case.

c) Beam arm resolution

We think that the layout can still be improved; we weren't able to achieve such a large dispersion as in the SA without getting into a series of aberrations of various kind. So whereas the X magnification in both layouts is roughly the same as in the SA, the dispersion from IT to DHF2 is roughly 4 instead of 8. One can use better detectors, however (200 μ resolution for instance) if one can have a smaller initial beam, i.e. a smaller IT, which we fixed at 1 mm in diameter. For example from DHF2 to ET (in which the X coordinate will be essentially o or very small) we have for layout 1 :

$$X_T \simeq 0 = -1.224\, X - 4.620\, \delta \quad ,$$

and for layout 2 :

$$X_T \simeq 0 = 1.872\, X - 8.429\, \delta \ ,$$

which means for layout 1 :

$$\delta = -\frac{1.224}{4.620}\, X_{DHF2} = -0.265\, X_{DHF2}$$

and for layout 2 :

$$\delta = \frac{1.872}{8.429}\, X_{DHF2} = 0.222\, X_{DHF2} \quad ,$$

so we can see that we don't have very different values, and as a first approximation (a more refined computation should take into account finite beam size and 3^{rd} order optical corrections) we can see that a 1 mm X resolution in DHF2 reflects itself in a 0.025 % resolution in momentum in the ET.

We considered up to now the BA and the SA as two separate entities with separate acceptances and resolutions. This is not true, however, if we combine the BA and the SA in a single instrument, we can see that we have a poor phase space matching at the external target: so, even if the SA itself is capable of a high resolution and high acceptance, the beam phase space at the ET is worsening the situation. We were unable at this stage of the work to design a BA with a smaller phase space at the ET but we hope that in further refinaments of the project this will be certainly possible.

We give here the situation of what happens in the SA when exact phase space matching is imposed in the ET: the transport matrices obviously do not change, so we will give only the situation of beam vectors, acceptances and resolutions.

a) Layout 1 :

New beam vectors are :

From (ET) (see 6.1)

(0.101 0.612 0.168 0.447 1.0)

From the triplet lens (see 6.3)

(1.999 0.031 0.510 0.149 1.0) .

We can see that even in this case, at the expense of losing some of the beam, we can do Cerenkov separation.

From SP1 (see 6.5)

(3.633 1.200 1.021 0.147 1.0)

From SL2 (see 6. 6)

(4. 934   0. 580   1. 048   0. 101   1. 0)

From SP2 (see 6. 7)

(8. 002   0. 838   0. 787   0. 102   1. 0)

The resolution of the SA (see 7. 6) can be computed at the focus as

$$X = 1.733 \cdot 0.101 + 8$$

with   0. 02 at 400 GeV/c. This gives

$$X = 0.18 + 0.16 .$$

In this case we can see that the contributions from the finite target size and the momentum dispersion are of the same order of magnitude : this means that we must arrange our detectors in such a way as to have the possibility of computing also the transverse (x and y) coordinates at the ET. The "direct reading" of the momentum at the focus has to be intended only as a rough approximation of the true momentum.

b) Layout 2 :

The beam vectors in this case are :

From ET (see 6. 1)

(0. 173   0. 291   0. 485   0. 165   1. 0)

From the triplet lens SL1 (see 6. 3)

(0. 952   0. 053   0. 468   0. 430   1. 0) .

We can see here that Cerenkov analysis would be difficult in this case : this is no surprise, however, as we developed the layout 2 for futurible detectors less critically sensitive to angles (transition radiation or others).

From SP1 (see 6. 5)

(3. 189   1. 200   2. 574   0. 424   1. 0)

From SL2 (see 6. 6)

(4. 726   0. 490   2. 748   0. 105   1. 0)

From SP2 (see 6. 7)

(8. 006   0. 778   2. 271   0. 108   1. 0) .

The situation for what the resolution is concerned is not much different as for layout 1.

We have a warning to give to the reader who would try to invert the transport matrices (see Sect. 7) : they are extremely difficult to invert with the traditional pivotal method even in double precision so we used the algebraic-complement method, which comes out with extremely simple formulas A matrix A (disregarding the "1" information) is of the form

$$A = \begin{pmatrix} a_1 & a_2 & 0 & 0 & c_1 \\ a_3 & a_4 & 0 & 0 & c_2 \\ 0 & 0 & b_1 & b_2 & 0 \\ 0 & 0 & b_3 & b_4 & 0 \\ 0 & 0 & 0 & 0 & 1 \end{pmatrix}$$

So, if we put

$$\Delta_1 = \begin{vmatrix} a_1 & a_2 \\ a_3 & a_4 \end{vmatrix}, \qquad \Delta_2 = \begin{vmatrix} b_1 & b_2 \\ b_3 & b_4 \end{vmatrix}$$

we get

$$A^{-1} = \begin{pmatrix} \frac{a_4}{\Delta_1} & -\frac{a_2}{\Delta_1} & 0 & & \frac{a_2 c_2}{\Delta_1} - \frac{a_4 c_1}{\Delta_1} \\ -\frac{a_3}{\Delta_1} & \frac{a_1}{\Delta_1} & 0 & & \frac{a_3 c_1}{\Delta_1} - \frac{a_1 c_2}{\Delta_1} \\ 0 & 0 & \frac{b_4}{\Delta_2} & -\frac{b_2}{\Delta_2} & 0 \\ 0 & 0 & -\frac{b_3}{\Delta_2} & \frac{b_1}{\Delta_1} & 0 \\ 0 & 0 & 0 & & 1 \end{pmatrix}$$

8. - COULOMB SCATTERING. -

This is a kind of disturbing issue : from one side the MCS is very important because it poses a limit to the overall performance of an apparatus like this, based on a precise tracing of the particle trajectory; from another side, in a feasibility study it's more than impossible to evaluate its contribution, strictly dependent as it is from the kind and quantity of material crossed by the beam.

We will therefore only note that an apparatus like this, working at a momentum roughly twice as high as the FNAL spectrometer, should show a $\langle \theta_c \rangle$ roughly one half. The overall lengths of the two apparatus are quite similar, so we can expect also the spread in the coordinates from MCS ΔX_c, ΔY_c seen by our apparatus to be one half of those seen at FNAL. Therefore the MCS should have roughly the same influence in the t resolution as it has at FNAL. We don't think that we can say anything more specific at this stage.

9. - CONCLUSIONS. -

We do think that with superconducting elements an FSAS could be built, with no more difficulties than those which were already overcome at FNAL. Future studies, starting from this very preliminary sketch could improve several features and may also allow to push the instrument to even higher energies.

We do think that in a line of thought that sees this as a part of a general purpose equipment one could also consider the possibility of surrounding the ET with some exclusive reactions detector, such as a Omega - like device.

We will continue to develop this project and we will be most grateful to all our colleagues that will collaborate to this design and that will send us suggestions and/or criticisms which will be equally welcome.

REFERENCES. -

(1) - K. Brown et al., SLAC Report no. 75 (1975).

(2) - C. Favuzzi and F. Waldner, Inclusive reactions kinematics $p+p \rightarrow \begin{pmatrix}\pi \\ K \\ p\end{pmatrix} + X$, (t, mm) vs ($\theta$, p_3), Report INFN/AE-75/10 (1975).